

Chaotic-Integrable Transition for Disordered Orbital Hatsugai-Kohmoto Model

Ying-Lin Li^a ¹, Chen-Te Ma^b ², and Po-Yao Chang^a ³

^a *Department of Physics, National Tsing Hua University, Hsinchu 30013, Taiwan.*

^b *Department of Physics and Astronomy, Iowa State University, Ames, Iowa 50011, US.*

Abstract

We have drawn connections between the Sachdev-Ye-Kitaev model and the multi-orbit Hatsugai-Kohmoto model, emphasizing their similarities and differences regarding chaotic behaviors. The features of the spectral form factor, such as the dip-ramp-plateau structure and the adjacent gap ratio, indicate chaos in the disordered orbital Hatsugai-Kohmoto model. One significant conclusion is that the plateau value of the out-of-time-order correlator, whether in the Hatsugai-Kohmoto model, Sachdev-Ye-Kitaev model with two- or four-body interactions, or a disorder-free Sachdev-Ye-Kitaev model, does not effectively differentiate between integrable and chaotic phases in many-body systems. This observation suggests a limitation in using out-of-time-order correlator plateau values as a diagnostic tool for chaos. Our exploration of these ideas provides a deeper understanding of how chaos arises in non-Fermi liquid systems and the tools we use to study it. It opens the door to further questions, particularly about whether there are more effective ways to distinguish between chaotic and integrable phases in these complex systems.

¹e-mail address: s1012424@gmail.com

²e-mail address: yefgst@gmail.com

³e-mail address: pychang@phys.nthu.edu.tw

1 Introduction

Non-Fermi liquids (NFLs) are characterized by the absence of well-defined quasiparticles, distinguishing them from Fermi liquids. The notable NFL models such as the *Sachdev-Ye-Kitaev* (SYK) model [1, 2] and the multi-channel Kondo impurity (MCKI) model, both of which exhibit chaotic behavior [2, 3, 4, 5].

Recently, renewed interest has emerged in a class of exactly solvable many-body fermionic models with infinite-range interactions, initially proposed by Hatsugai and Komohto (HK) [6]. It has been found that the ground states of the HK model do not exhibit the characteristics of Fermi liquids. By introducing an energy cost U for double occupancy in each momentum state, the HK model can be expressed as:

$$H_{\text{HK}} = \sum_{k\sigma} \varepsilon_k n_{k\sigma} + U \sum_k n_{k\uparrow} n_{k\downarrow}. \quad (1)$$

Here ε_k denotes the dispersion in a tight binding model with no orbital degrees of freedom, with the band index k in the one-dimensional Brillouin zone (BZ), and $\sigma = \uparrow, \downarrow$ indicates the z -component of the electron spin. The number operator is defined as

$$n_{\alpha,\sigma} = c_{\alpha,\sigma}^\dagger c_{\alpha,\sigma} \quad (2)$$

under the many-body basis. This paper considers HK-type interactions that impose an energy penalty on doubly-occupied orbital degrees of freedom α . An extension of the HK model, which includes an orbital term [7]

$$H_{\text{OHK}} = \sum_{k,\alpha<\alpha',\sigma} (t_{\alpha\alpha'\sigma}(k) c_{k\alpha\sigma}^\dagger c_{k\alpha'\sigma} + \text{H.C.}) - \mu \sum_{k,\alpha} n_{k\alpha\sigma} + \sum_{k,\alpha,\alpha'} U_{\alpha\alpha'}(k) n_{k\alpha\uparrow} n_{k\alpha'\downarrow}, \quad (3)$$

where we assume

$$U_{\alpha,\alpha'}(k) = U_{k,\alpha} \delta_{\alpha,\alpha'} \quad (4)$$

respecting the Pauli principle. The chemical potential is set to zero for simplicity, i.e., $\mu = 0$. We adjust the permissible orbital number in the half-filling scenario with zero total spin. Extending the HK model to include orbital degrees of freedom preserves its non-fermi liquid behavior. The solvability of the HK model arises from its locality in momentum space. However, when viewed in position space, the interaction term becomes highly non-local, coupling *position-space* points through a four-point function. This is similar to the SYK model with a four-body interaction (SYK₄ model). Exploring the chaotic phenomena of the orbital HK model is significant.

In classical mechanics, chaotic systems are highly *sensitive* to initial conditions, a phenomenon captured by the exponential divergence of nearby trajectories. However, due to the uncertainty principle, quantum systems governed by wavefunctions and probabilities do not allow for the same kind of trajectory-based analysis. The difficulty arises because, taking the limit where $\hbar \rightarrow 0$ and the system's non-integrability parameter (which measures how far the system is from being integrable) becomes small, do *not* commute [8]. This lack of commutativity means that simply shrinking \hbar does not smoothly lead to the classical chaotic behavior one might expect. This discrepancy complicates efforts to explain classical chaos in a quantum framework. While quantum systems *cannot* exhibit classical chaos in the traditional sense (because their evolution is deterministic via the Schrödinger equation), they do exhibit quantum signatures of chaos, such as:

- **Energy Level Statistics:** In chaotic quantum systems, the distribution of energy levels tends to follow the predictions of random matrix theory (RMT) [9], in contrast to the regular, predictable spacing seen in integrable systems [10].
- **Wavefunction Behavior:** Chaotic quantum systems can display complicated, highly irregular wavefunctions, contrasting with the regular patterns seen in non-chaotic systems [11].
- **Quantum Scars:** In some cases, wavefunctions of quantum chaotic systems can show localized structures along classical periodic orbits, known as "quantum scars".

One popular approach to studying quantum chaos involves semi-classical methods, which attempt to bridge the gap between quantum and classical descriptions [12]. Gutzwiller's trace formula is an example of relating quantum energy levels to classical periodic orbits [12].

In the context of quantum chaos, RMT provides a statistical framework to understand the energy level distribution in quantum systems, especially those that exhibit chaotic behavior [13]. In integrable quantum systems (those that have regular, predictable behavior), energy levels tend to cluster in a Poissonian distribution, meaning the gaps between levels are random and independent [13]. However, in chaotic quantum systems, the energy levels tend to avoid each other, leading to *level repulsion* [13]. The distribution of energy level spacings in such systems follows the Wigner-Dyson distribution

(from RMT) [14]. This describes the probability of finding two nearby energy levels at a certain distance apart. The distribution is typical of random matrices that are either:

- Orthogonal Ensemble (if the system respects time-reversal symmetry);
- Unitary Ensemble (if the system breaks time-reversal symmetry);
- Symplectic Ensemble (for systems with additional symmetries like spin-orbit coupling).

For example, for the Gaussian orthogonal ensemble (GOE), the level spacing follows

$$P(s) = \frac{\pi s}{2} \exp\left(-\frac{\pi s^2}{4}\right), \quad (5)$$

where s is the normalized spacing between neighboring energy levels. This distribution shows a low probability of two energy levels being very close together or far apart, with a peak indicating some typical spacing between levels.

The distribution of energy levels provides the uniquely chaotic properties in a many-body quantum system. Currently, we lose a general method to study quantum chaos in a few-body system [15]. Hence, diagnosing quantum chaos is still challenging. Another diagnostic method from the energy spectrum is the spectral form factor (SFF), which is the square of the Fourier transform of the empirical spectral density [16, 17]. With the disorder average, the SFF (g), the disconnected part (g_d) and the connected part (g_c) are defined:

$$g(t, \beta) \equiv \frac{\langle Z(\beta, t) Z^*(\beta, t) \rangle_{t_h, U}}{\langle Z(\beta) \rangle_{t_h, U}^2}; \quad (6)$$

$$g_d(t, \beta) \equiv \frac{\langle Z(\beta, t) \rangle_{t_h, U} \cdot \langle Z^*(\beta, t) \rangle_{t_h, U}}{\langle Z(\beta) \rangle_{t_h, U}^2}; \quad (7)$$

$$g_c(t, \beta) \equiv g(t, \beta) - g_d(t, \beta) \quad (8)$$

in terms of the partition function, which is the trace of the time-evolved and thermally weighted Hamiltonian [18]

$$Z(\beta, t) \equiv \text{Tr}(e^{-\beta H - iHt}), \quad (9)$$

where the inverse temperature is β . The disorder average $\langle \cdot \rangle_{t_h, U}$ ensures that the SFF is averaged over an ensemble of random couplings (t_h and U).

In chaotic quantum systems, the SFF is expected to display the characteristic "dip-ramp-plateau" structure [16, 17, 18]. Initially, the SFF decreases (dip) due to interference between energy levels. As the system evolves, the SFF ramps up, reflecting the emergence of a correlation between energy levels. Eventually, it reaches a plateau, indicating the saturation of correlations, a feature of quantum chaos. The disorder parameter or randomness can generate the shape of the SFF in an integrable system [19, 20]. Therefore, the SFF's shape alone is insufficient to uniquely diagnose quantum chaos [19, 20]. This limitation suggests that other spectral observables or diagnostics are necessary to capture the few-body systems' chaotic dynamics fully.

We discuss the role of sensitivity to initial conditions and out-of-time-order correlations (OTOCs) in distinguishing chaotic and integrable systems, particularly in quantum many-body systems. While sensitivity to initial conditions is often associated with chaos (as in classical chaos theory), it alone is *insufficient* to differentiate chaotic systems from integrable ones. The system's dynamics can still exhibit sensitivity to initial conditions in integrable systems. However, they do *not* exhibit the irregular behavior typical of chaos [21]. OTOCs are

$$C(t) = \langle [V(0), W(t)][W^\dagger(t), V^\dagger(0)] \rangle \geq 0, \quad (10)$$

where $W(t)$ and $V(t)$ are operators in the Heisenberg representation, and the angle bracket denotes the thermal average are a diagnostic tool for detecting the chaotic features in quantum systems. These correlation functions reflect how operators evolve and fail to commute over time. In the context of chaos, OTOCs show exponential growth, a hallmark of chaotic behavior. In the semi-classical limit, OTOCs exhibit exponential growth up to a time scale known as the Ehrenfest time. The growth rate is characterized by the Lyapunov exponent λ_L (the exponent of the OTOCs when it is non-negative), which measures how rapidly initial perturbations grow over time. In some cases, such as the SYK model, the Lyapunov exponent reaches a theoretical upper bound [2, 22]. The disorder-free SYK model [20] though *not* having random matrix behavior, still shows chaotic characteristics with a *non-zero* Lyapunov exponent when the system size is large enough [23]. Introducing disorder into systems can induce chaotic behavior. However, it is *essential* to differentiate this induced randomness from inherent quantum chaos [19, 20]. The presence of randomness does *not* necessarily mean that the system is chaotic. In general, exchanging the logarithm and the thermal average influences the Lyapunov exponent [24]. Therefore, the Lyapunov exponent generally depends on regularization, *unless* considering a many-body system. The late-time be-

havior of OTOCs, precisely the plateau value of the correlation function, is a topic of ongoing investigation [25]. It could serve as an indicator of chaos in general systems, but questions remain about whether this plateau is merely a finite-size artifact or holds deeper physical meaning.

This paper examines chaotic behaviors in non-Fermi liquid systems, specifically focusing on the disordered orbital HK model. By introducing disorder to the model as that $t_{\alpha\alpha'\sigma}(k)$ (t_h) and $U_{k,\alpha}$ (U) follow the Gaussian distribution with the zero mean and the variance of t_h and U can be tuned and studying statistical distributions, the paper provides insights into how chaos emerges. After the Fourier transformation to the position space, the disordered orbital HK model is similar to the SYK₂+SYK₄ model. Key points include using the adjacent gap ratio and spectral form factor to characterize chaos and transition between integrable and chaotic phases. The paper also calculates OTOCs to explore the impact of regularization on late-time behavior by comparing the disordered orbital HK model to the SYK₂, SYK₄, and disordered-free SYK models. Our paper enhances our understanding of chaos in disordered non-Fermi liquids, particularly through the novel application of statistical tools like the adjacent gap ratio, the SFF, and OTOCs to probe the late-time scale. To summarize our results:

- A phase diagram for the variances of the disorder parameters, t_h and U , is constructed using the adjacent gap ratio in the disordered orbital HK model. This model has the GOE by turning on the four-point term. The SFF is consistent with the presence of chaos in the disordered orbital HK model.
- The plateau value of the OTOCs varies depending on regularization, indicating that the late-time behavior of the system is sensitive to how regularization is handled. Unlike the early-time regime, the temperature dependence at late times does not differentiate between integrable and chaotic behavior.

The organization of this paper is as follows: In Sec. 2, we introduce the disordered orbital HK model. In Sec. 3, we study the spectral statistics by calculating the adjacent gap ratio and the spectral form factor. Sec. 4 explores the late-time scale of the OTOCs. Finally, we present our concluding remarks in Sec. 5.

2 Disordered Orbital HK Model

The Hamiltonian of the disordered orbital HK model, after Fourier transformation

$$c_{x_1\alpha\sigma}^\dagger = \sum_{k \in \text{BZ}} e^{ikx_1} c_{k\alpha\sigma}^\dagger, \quad (11)$$

is given by

$$\begin{aligned} & H_{\text{OHK}} \\ = & \sum_{x_1, 2, \alpha < \alpha', \sigma} \sum_k t_{k\alpha\alpha'\sigma} e^{ik(x_1-x_2)} c_{x_1\alpha\sigma}^\dagger c_{x_2\alpha'\sigma} + \text{H.C.} \\ & + \sum_{x_1, 2, 3, 4\alpha} \sum_k U_{k\alpha} e^{ik(x_1-x_2+x_3-x_4)} c_{x_1\alpha\uparrow}^\dagger c_{x_2\alpha\uparrow} c_{x_3\alpha\downarrow}^\dagger c_{x_4\alpha\downarrow}, \end{aligned} \quad (12)$$

where x_1, x_2, x_3, x_4 label position space lattice point. Therefore,

$$\sum_k t_{k\alpha\alpha'\sigma} e^{ik(x_1-x_2)}; \quad \sum_k U_{k\alpha} e^{ik(x_1-x_2+x_3-x_4)} \quad (13)$$

play the role of random variables for two-point and four-point functions in a real space, respectively. This model is analogous to the SYK₂+SYK₄ model, described by the Hamiltonian

$$H_{\text{SYK}_2+\text{SYK}_4} = \frac{i}{2!} \sum_{i_1, i_2=1}^N \kappa_{i_1 i_2} \chi_{i_1} \chi_{i_2} + \frac{1}{4!} \sum_{i_1, i_2, i_3, i_4=1}^N J_{i_1 i_2 i_3 i_4} \chi_{i_1} \chi_{i_2} \chi_{i_3} \chi_{i_4}, \quad (14)$$

where χ_{i_1} represents Majorana fermions, and the random couplings J_{ijkl} and κ_{ij} follow the Gaussian distribution with the zero mean and the standard deviations $\sqrt{6}J/N^{3/2}$ and κ/\sqrt{N} , respectively. We can generally set the fixed-coupling constant J as one because the results only depend on the ratio of two fixed coupling constants J and κ . We define N as the number of Majorana fermion fields. The two-body interaction term is called the SYK₂ model, and another four-body interaction is called the SYK₄ model. A chaotic-integrable transition has been observed in the SYK₂+SYK₄ model [10]. This raises the question of whether a similar transition might occur in the disordered orbital HK model.

Before proceeding with our chaos analysis, we first summarize the known, unknown results, and our results in the non-Fermi liquid models and the related models that we will consider in the tabel 1. The disorder-free SYK model [20] is the SYK₄ model with

Model	Adjacent Gap Ratio	SFF	Early-Time OTOCs	Late-Time OTOCs
SYK ₂	Poisson [10]	no linear ramp [20]	constant in time [10]	β ind.
SYK ₄	all random matrix [4]	dip-ramp-plateau [4]	exponential growth [10]	β ind.
Disorder-Free SYK	Poisson [20]	no linear ramp [20]	exponential growth [23]	β ind.
MCKI	?	?	exponential growth [5]	?
Disordered Orbital HK	GOE and Poisson	dip-ramp-plateau (GOE) and no linear ramp (Poisson)	?	regularization dep.

Table 1: Chaotic properties of various non-Fermi liquid models and related models.

the uniform distribution [23]

$$J_{i_1 i_2 i_3 i_4} = 1. \quad (15)$$

The operators of the OTOCs in the SYK₂, SYK₄, and disorder-free SYK models are the Majorana fermions. While in the disorder orbital HK model, the operator of the OTOC is the number operator.

3 Spectral Statistics

We study the spectral statistics of the disordered orbital HK model by calculating the average adjacent gap ratio [14] through the exact diagonalization. The phase diagrams for the variances of the t_h and U show the GOE and Poisson regimes. The transition between chaotic and integrable behavior is observed. The SFF [16] demonstrates the dip-ramp-plateau behavior in the GOE regime, which supports our observation.

3.1 Adjacent Gap Ratio

To analyze the level statistics, we first collect the eigenenergies E_n and arrange them in ascending order

$$E_1 < E_2 < \dots . \quad (16)$$

We define the level spacing as

$$\Delta E_n = E_{n+1} - E_n, \quad (17)$$

and the ratios of adjacent level spacings are given by

$$r_n = \frac{\Delta E_n}{\Delta E_{n+1}}. \quad (18)$$

In a generic integrable system, the energy levels are uncorrelated such that the probability distribution of r_n follows the Poisson distribution,

$$p_p(r_n) = \frac{1}{(1+r_n)^2}. \quad (19)$$

For a quantum chaotic system, the energy levels repel each other, resulting in a probability distribution that follows Wigner-Dyson (WD) statistics [12, 13],

$$p_W(r_n) = \frac{1}{A_\nu} \frac{(r_n + r_n^2)^\nu}{(1 + r_n + r_n^2)^{1+1.5\nu}}, \quad (20)$$

where ν and A_ν are constants depending on the ensemble symmetries [9]:

- Gaussian Orthogonal Ensemble (GOE): $\nu = 1, A_1 = 8/27$;
- Gaussian Unitary Ensemble (GUE): $\nu = 2, A_2 = 4\pi$;
- Gaussian Symplectic Ensemble (GSE): $\nu = 4, A_4 = 4\pi/(729\sqrt{3})$.

We present the probability distribution of the logarithmic ratio $\ln r_n$, which is given by

$$P(\ln r_n) = p(r_n)r_n, \quad (21)$$

see Figs. 1a and 1b. In the figures, we remove the subscript n for r_n for the convenient reading. As the system approaches chaotic behavior, the distribution tends to resemble the GOE distribution, consistent with our Hamiltonian preserving real symmetric properties.

The adjacent gap ratio is defined as

$$\tilde{r}_n = \frac{\min(r_{n-1}, r_n)}{\max(r_{n-1}, r_n)}. \quad (22)$$

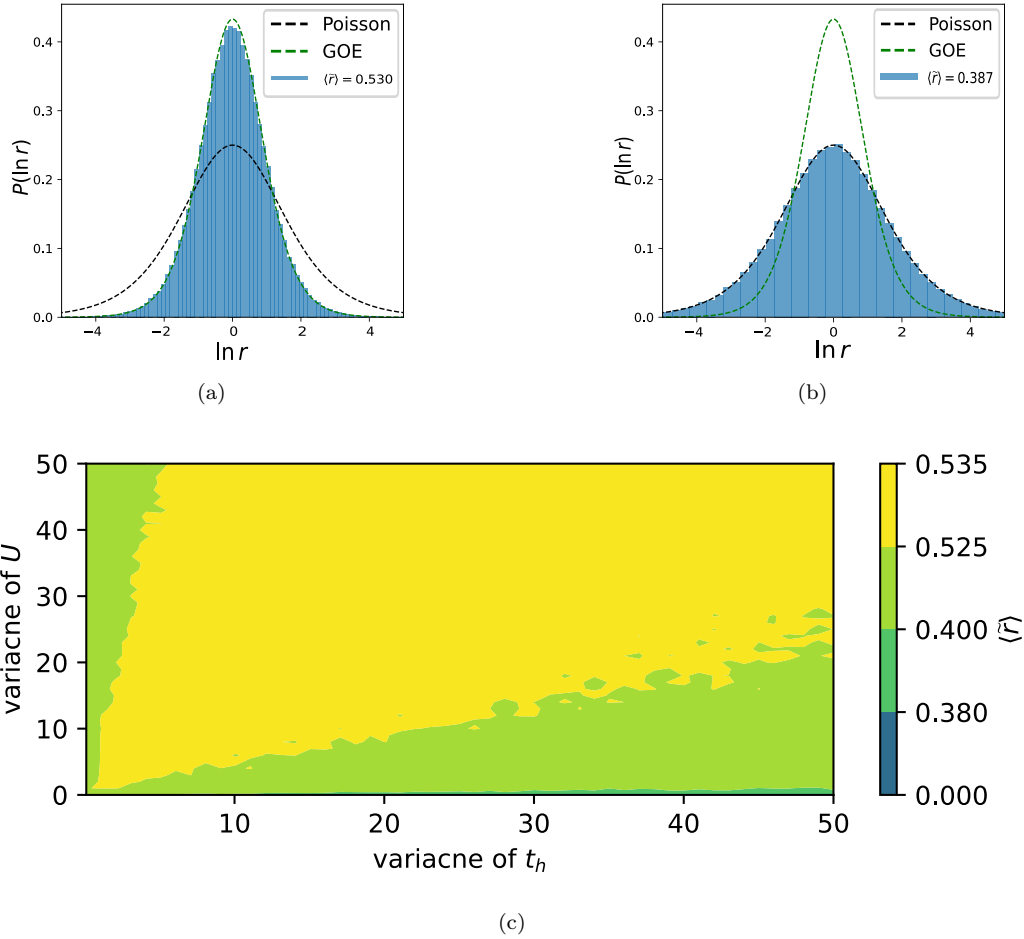


Figure 1: Logarithmic ratio distribution of $\ln r$ over 100 random samples for the disordered orbital HK model with 8 orbitals with half-filling and 0 total spin. (a) Chaotic phase with $\langle \tilde{r} \rangle = 0.530$, $\langle t_h^2 \rangle = 1$, and $\langle U^2 \rangle = 3.3$. (b) Integrable phase with $\langle \tilde{r} \rangle = 0.387$, $\langle t_h^2 \rangle = 1$, and $\langle U^2 \rangle = 0$. (c) Phase diagram of the average adjacent gap ratio as a function of t_h and U (varied in 0.5 units) over 50 random samples.

After averaging the adjacent gap ratio, a Poisson distribution gives [14]

$$\langle \tilde{r} \rangle \approx 0.387 \quad (23)$$

whereas for GOE [14]

$$\langle \tilde{r} \rangle \approx 0.531. \quad (24)$$

As shown in Fig. 1c, the phase diagram of $\langle \tilde{r}_n \rangle$ indicates the Poisson and GOE statistics with different variance of t_h and U . When the variance of U tends to zero, the system becomes integrable. When $\langle t_h^2 \rangle / \langle U^2 \rangle \approx 1/3.3$, the system tends towards GOE. These

results indicate that the distribution aligns with RMT predictions. Moreover, as seen in Fig. 2, we compute a system’s average adjacent gap ratio by allowing 2, 4, 6, and 8 orbital numbers. We observe that the integrable regime vanishes, and the $\langle \tilde{r} \rangle$ value approaches the GOE value if we turn on the four-point term when the allowable orbital number becomes more considerable. A subtle distinction arises between the vanishing limit of the variance of U and t_h . When allowing infinite orbital numbers, while the system reaches the integrable regime as the variance of U vanishes first, it enters the GOE regime when the variance of t_h approaches zero first.

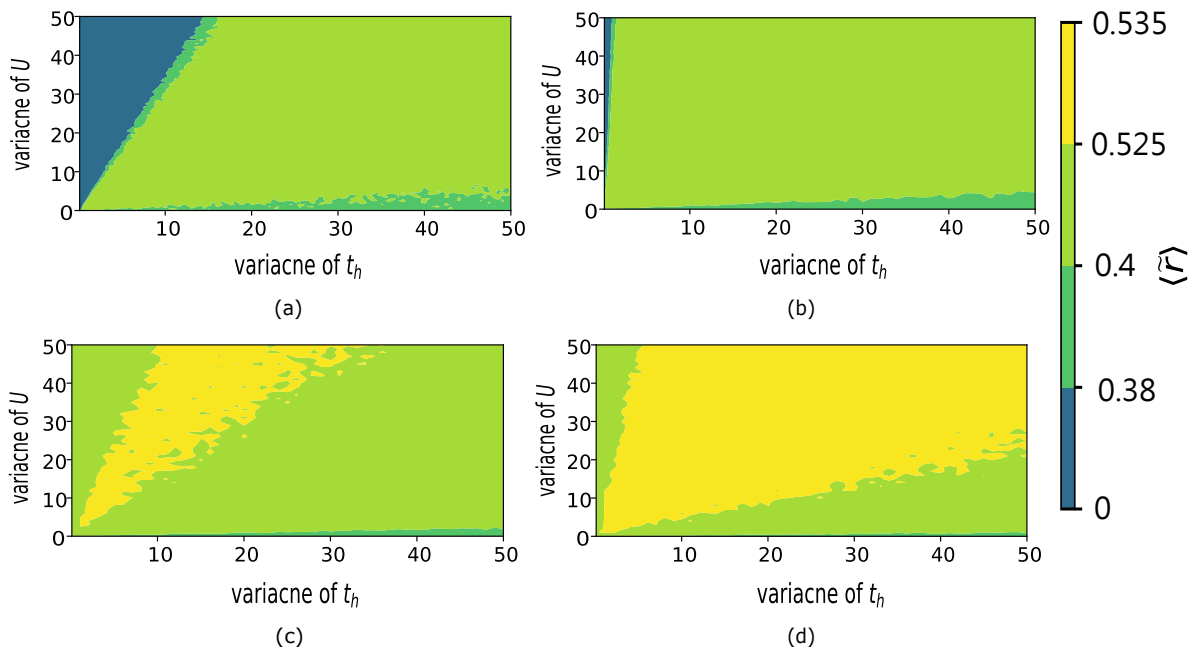


Figure 2: Phase diagrams showing the average adjacent gap ratio as a function of t_h and U , both varied in 0.5 unit intervals: (a) 2 orbitals with results averaged over 2000 random samples; (b) 4 orbitals with 1000 random samples; (c) 6 orbitals with 100 random samples; (d) 8 orbitals with 50 random samples.

3.2 Spectral Form Factor

While the level spacing statistic provides valuable GOE, the SFF helps offer supporting information. The ramp feature observed in the SFF is attributed to long-range level repulsion [4, 17]. When balanced against the effects that keep the energy finite, this repulsion gives rise to a less rigid eigenvalue structure. Consequently, due to its low rigidity, the SFF exhibits a ramp-shaped increase that linearly grows over time before

transitioning into a plateau. Note that $g(t)$ is dominated by the disconnected SFF $g_d(t)$ before the dip time and by the connected SFF $g_c(t)$ after the dip time. In Ref. [4], a dip-ramp-plateau behavior was observed for the SYK model, particularly in the ramp and plateau regions, with a subtle difference in early-time behavior. For the disordered orbital HK model, the unfolded SFF patterns in integrable and chaotic cases at infinite temperature fall between the Poisson and GOE predictions of RMT, as shown in Fig. 3.

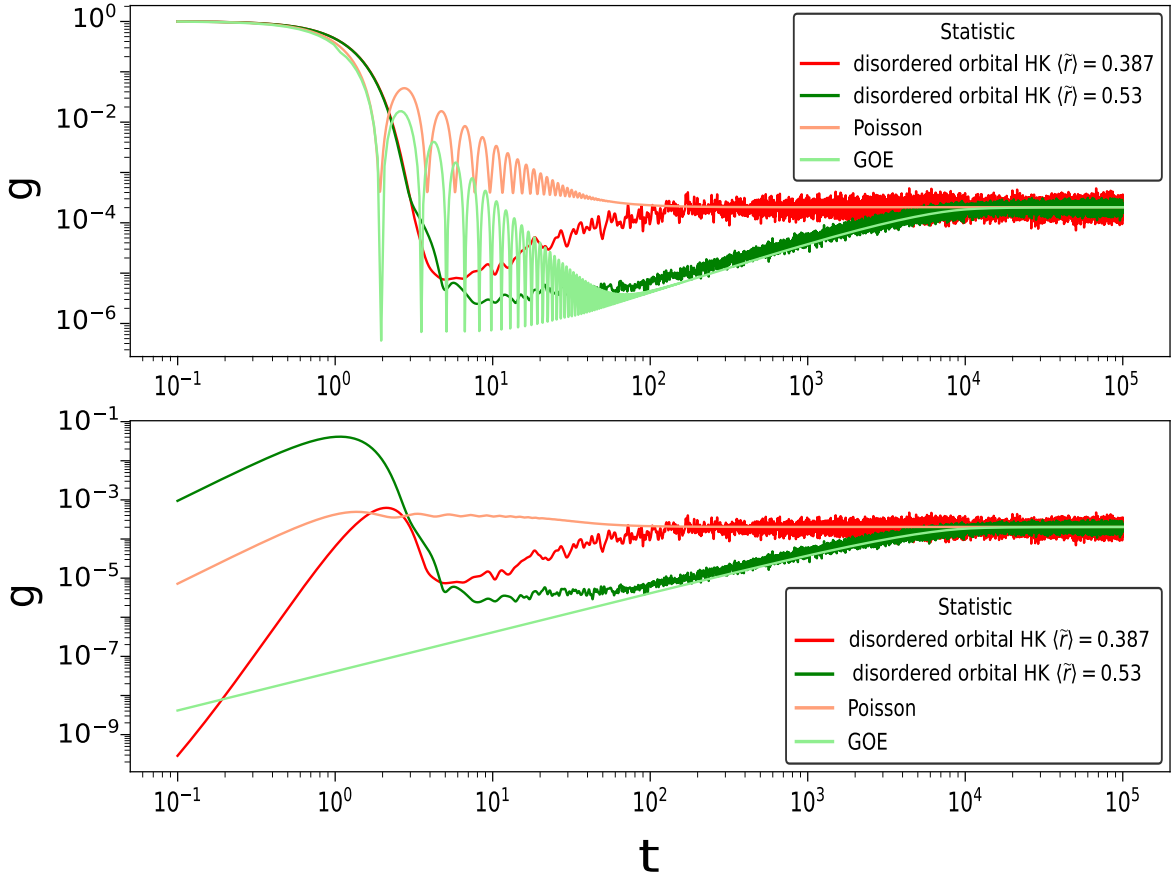


Figure 3: SFF for infinite temperature, averaged over 50 random samples for the disordered orbital HK model with 8 orbitals with half-filling and 0 total spin. The chaotic phase is characterized by $\langle \tilde{r} \rangle = 0.53$ with $\langle t_h^2 \rangle = 1$ and $\langle U^2 \rangle = 3.3$, and the integrable phase by $\langle \tilde{r} \rangle = 0.387$ with $\langle t_h^2 \rangle = 1$ and $\langle U^2 \rangle = 0$. The unfolded SFF is displayed in the upper plot, while the connected portion is shown in the lower plot.

In the case where

$$\langle \tilde{r}_n \rangle = 0.53, \quad (25)$$

the SFF exhibits the characteristic dip-ramp-plateau structure. Furthermore, as seen in Fig. 4, with large orbitals considered, the SFF demonstrates the linear ramp as the theoretical prediction.

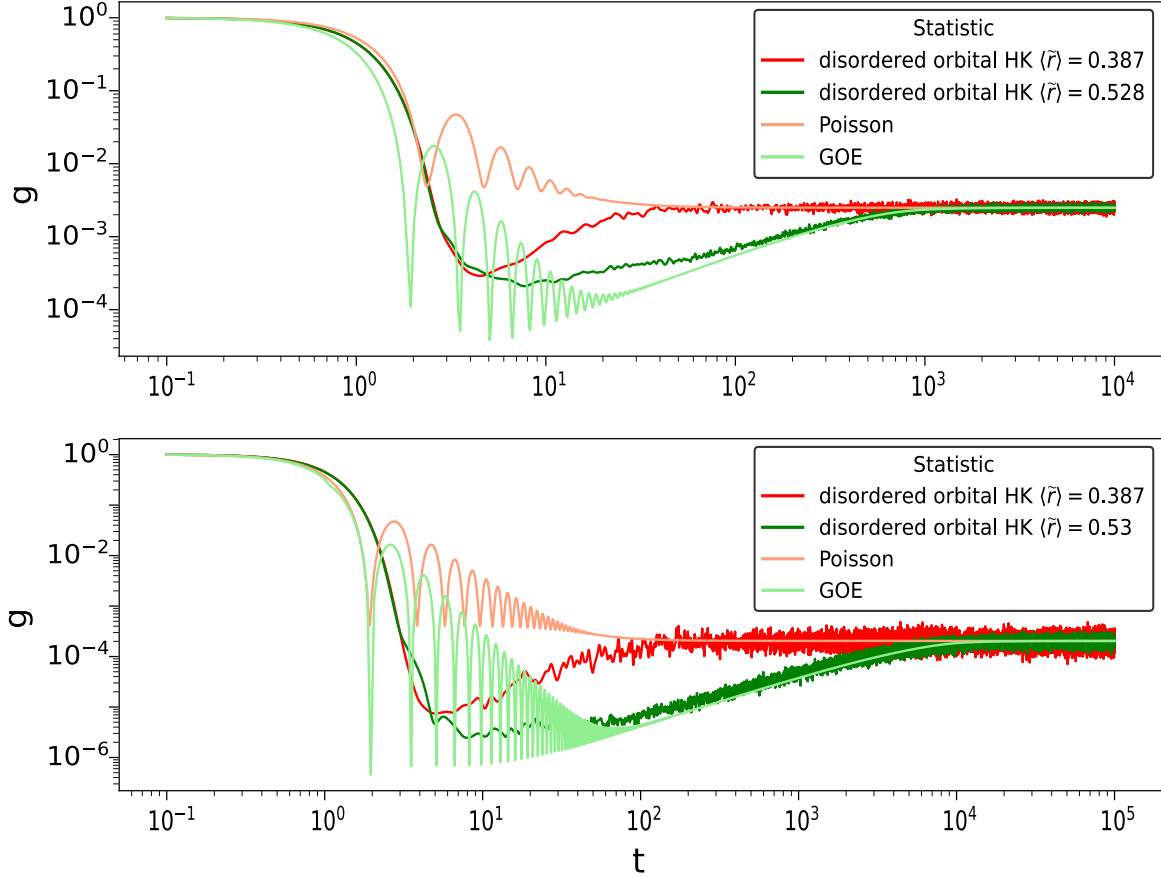


Figure 4: SFF at infinite temperature for the disordered orbital HK model with 6 and 8 orbitals at half-filling and zero total spin. The upper plot displays the results for the 6-orbital scenario, averaged across 500 random samples. The lower plot illustrates the 8-orbital scenario, averaged across 50 random samples.

4 OTOCs

To study the disordered orbital HK model, we choose operators as the number operators $n_{\alpha,\sigma}$ in the OTOCs

$$C(t) = \frac{1}{N_o(N_o - 1)} \sum_{n_{\alpha,\sigma} \neq n_{\alpha',\sigma'}} -\langle [n_{\alpha,\sigma}(0), n_{\alpha',\sigma'}(t)]^2 \rangle, \quad (26)$$

where N_o is the number of $n_{\alpha,\sigma}$. We calculate $C(t)$ by averaging over random samples $\langle C(t) \rangle_{t_h, U}$. As shown in the down plot of Fig. 5, in the Poisson distribution regime where $\langle t_h^2 \rangle = 1$ and $\langle U^2 \rangle = 0$, the OTOCs remain constant across different temperatures. However, in the GOE distribution regime, with $\langle t_h^2 \rangle = 1$ and $\langle U^2 \rangle = 3.3$, the late time behavior of OTOCs increases with temperatures, as illustrated in the up plot of Fig. 5. This behavior possibly arises from varying exponents during early times. Due to the numerical difficulties in calculating the Lyapunov exponent, the late-time behavior is particularly noteworthy.

Additionally, as depicted in Fig. 6, the system size does not affect the temperature-dependent late-time behavior of OTOCs. However, when we analyze the plateau values of OTOCs in other many-body models, such as the SYK₂ model, the disorder-free SYK model [20], and the SYK₄ model, we observe that the saturated values are temperature-independent across both integrable and maximally chaotic models, as illustrated in Fig. 7. Furthermore, we also examine the regularization issue through the regularized OTOCs,

$$F(t) = \text{Tr}(yV(0)yW(t)yV(0)yW(t)), \quad (27)$$

where y is defined by

$$y^A = \frac{1}{Z} e^{-\beta H}, \quad (28)$$

where

$$Z = \text{Tr}(e^{-\beta H}), \quad (29)$$

as shown in Fig. 7. The normalized $F(t)$, i.e., $F(t)/F(0)$, shows that the saturated values tend to exhibit similar behavior in the SYK₂, disorder-free SYK model, and SYK₄ models. This result aligns with the $C(t)$ calculation, suggesting that the relationship between the late-time behavior of OTOCs and temperature may not be a

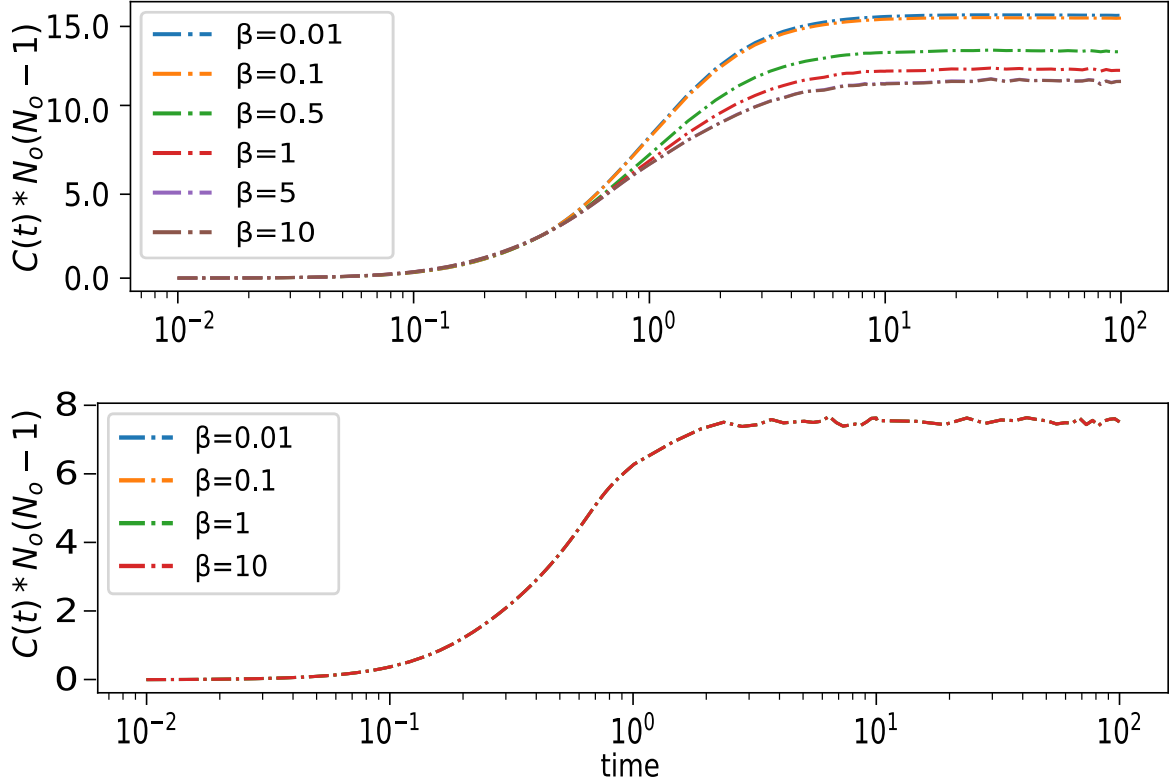


Figure 5: Results for 30 random samples with 6 orbitals. The OTOCs versus time on a log scale at different temperatures. The upper plot corresponds to GOE-level statistics with $\langle t_h^2 \rangle = 1$ and $\langle U^2 \rangle = 3.3$, while the lower plot represents Poisson-level statistics with $\langle t_h^2 \rangle = 1$ and $\langle U^2 \rangle = 0$. For the Poisson case, the OTOCs calculations are totally temperature independent. For the GOE case, the late-time values of OTOCs are temperature dependent. Note that $N_o = 12$.

reliable indicator of chaotic properties in many-body systems. However, a different behavior happens in the disordered orbital HK model. Therefore, the late-time OTOCs, in general, depends on the regularization.

5 Discussion and Conclusion

In this paper, we investigated the adjacent gap ratio (a measure of energy level repulsion) [14], spectral form factor [16], and out-of-time-order correlators in the disordered orbital HK model. The disordered orbital HK model, when Fourier transformed to

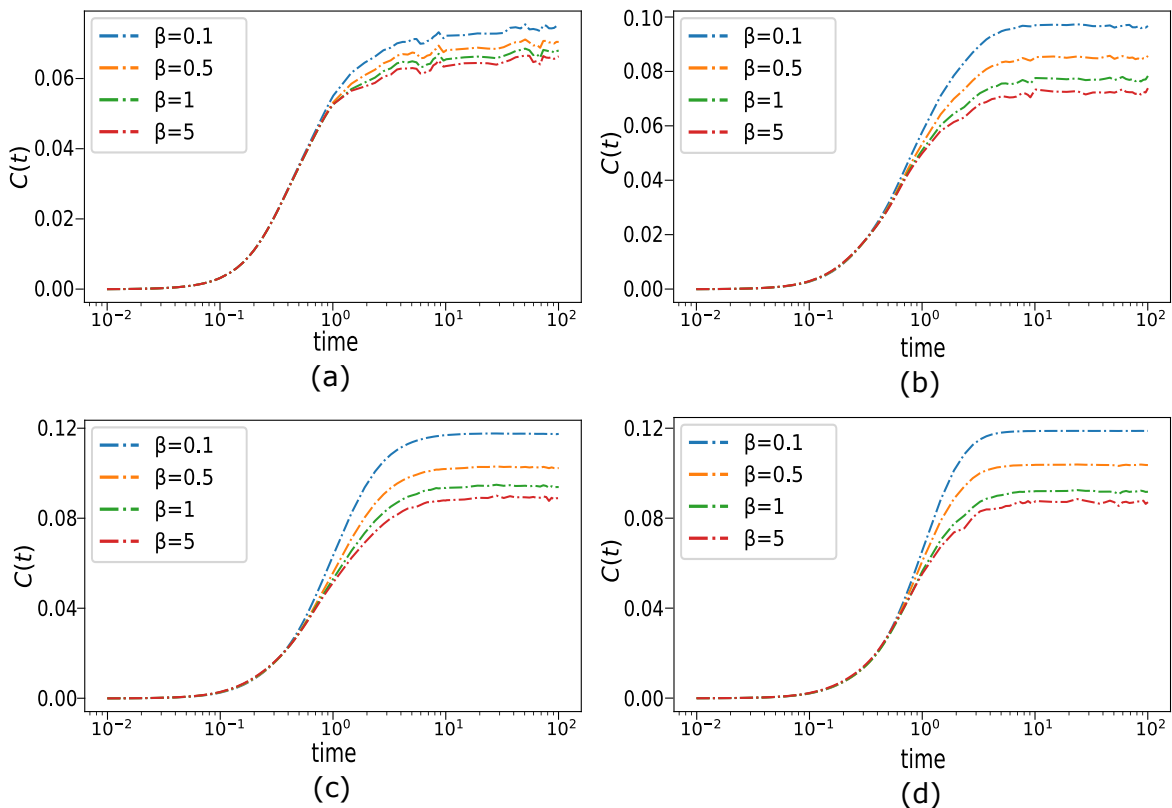


Figure 6: $C(t)$ calculation with different system size. (a) 2 orbitals with results averaged over 1000 random samples, (b) 4 orbitals with 100 random samples, (c) 6 orbitals with 30 random samples, (d) 8 orbitals with only 1 random sample. The results show that the system size does not affect the temperature-dependent late-time behavior of OTOCs.

position space, shows similarities to the $\text{SYK}_2 + \text{SYK}_4$ model [10], a well-known system for studying quantum chaos and integrability. Including the four-point interaction term in the adjacent gap ratio calculations reveals an increase in equity (presumably referring to a trend toward more universal chaotic behavior). SFF and OTOCs also corroborate this observation. SYK_2 and disorder-free SYK models exhibit temperature independence in late-time OTOC behavior, similar to the SYK_4 model. The disordered orbital HK model demonstrates dependence on regularization in its late-time behavior, suggesting that late-time OTOCs are not a reliable indicator of many-body chaos. This implies that using OTOC saturation values alone to distinguish between integrability and chaos may not always work.

We delved into an intriguing area of quantum chaos, particularly regarding the transition between chaotic and integrable behavior within quantum systems. Studying this

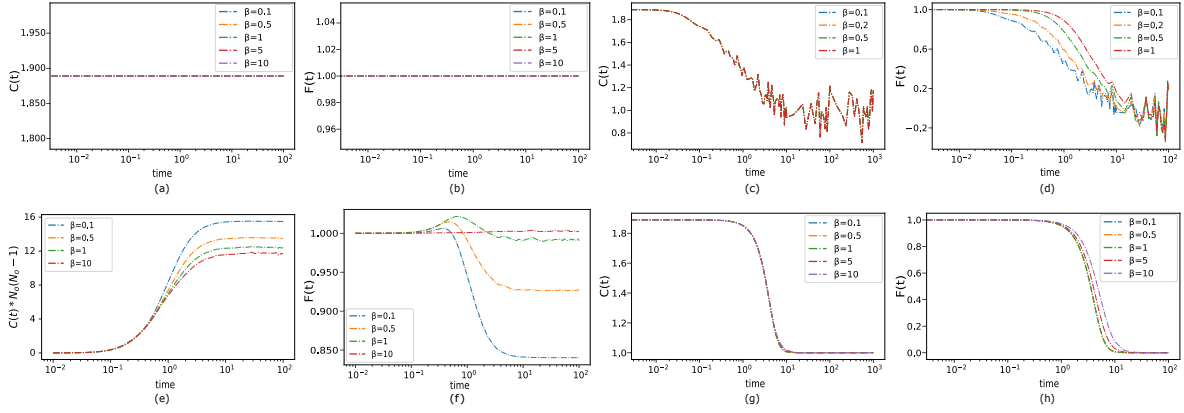


Figure 7: OTOCs calculations: $C(t)$ and normalized $F(t)$ for various models. (a)(b) SYK₂ model with $\kappa = 1$ and $N = 18$ over 10 random samples. (c)(d) Disorder-free SYK model with $N = 18$. (e)(f) Disordered orbital HK model with $\langle t_h^2 \rangle = 1$ and $\langle U^2 \rangle = 3.3$, considering 6 orbitals over 30 random samples. The number of number operators $N_o = 12$. (g)(h) SYK₄ model with $N = 18$ over 10 random samples.

transition through simpler models like the disordered orbital HK model is promising because it is less complex than models like the more involved SYK₂+SYK₄ model. In classical mechanics, integrable systems can be solved exactly, with as many conserved quantities as degrees of freedom, leading to regular, predictable motion. Chaotic systems, on the other hand, exhibit sensitive dependence on initial conditions and complex dynamics. Extending this distinction to quantum systems introduces a challenge, as quantum chaos needs a straightforward analog to classical chaos.

The HK model is a lattice-based system where electrons hop between orbitals in a disordered manner [6, 7], and can be modified with random variables to study NFL behavior and chaos. Unlike the SYK models [1], which are all-to-all interaction models (thus more complex to solve and numerically intensive), the disordered HK model's simplicity comes from local interactions on the momentum space, allowing us to track the onset of quantum chaos and integrability in a more manageable framework. By tuning the disorder or interaction strength in the disordered orbital HK model, we can induce a transition from integrable to chaotic behavior. This transition is essential for understanding quantum chaos in more complex systems, particularly NFLs. NFL behavior often arises in disordered systems, where quasiparticle descriptions break down. Understanding the chaotic regime could illuminate strongly correlated electron systems and unconventional superconductors. NFLs deviate from the conventional Fermi liquid theory by exhibiting non-quasiparticle excitations. The chaotic nature of some

NFLs suggests a deeper connection between chaos and the breakdown of conventional many-body theory. By studying the disordered orbital HK model, which might show NFL behavior under certain conditions, and comparing it with more complex models like SYK₂+SYK₄, we can explore how chaos influences the NFL state and its transitions. By bridging the chaotic-integrable transition using simpler models, our study can provide fresh insights into quantum chaos, offering a more intuitive understanding of how chaotic dynamics emerge even in systems with relatively few bodies. This has far-reaching implications for quantum information and condensed matter physics.

Acknowledgments

We would like to express our gratitude to Masaki Tezuka for his helpful discussion. CTM would thank Nan-Peng Ma for his encouragement. PYC acknowledges support from the National Science and Technology Council of Taiwan under Grants No. NSTC 113-2112-M-007-019. Both PYC and YLL thank the National Center for Theoretical Sciences, Physics Division for its support. CTM acknowledges the Nuclear Physics Quantum Horizons program through the Early Career Award (Grant No. DE-SC0021892).

References

- [1] A. Kitaev, “A simple model of quantum holography. - 2015,” Talks at KITP, April 7 and May 27.
- [2] J. Polchinski and V. Rosenhaus, “The Spectrum in the Sachdev-Ye-Kitaev Model,” *JHEP* **04**, 001 (2016) doi:10.1007/JHEP04(2016)001 [arXiv:1601.06768 [hep-th]].
- [3] A. M. García-García and J. J. M. Verbaarschot, “Spectral and thermodynamic properties of the Sachdev-Ye-Kitaev model,” *Phys. Rev. D* **94**, no.12, 126010 (2016) doi:10.1103/PhysRevD.94.126010 [arXiv:1610.03816 [hep-th]].
- [4] J. S. Cotler, G. Gur-Ari, M. Hanada, J. Polchinski, P. Saad, S. H. Shenker, D. Stanford, A. Streicher and M. Tezuka, “Black Holes and Random Matrices,” *JHEP* **05**, 118 (2017) [erratum: *JHEP* **09**, 002 (2018)] doi:10.1007/JHEP05(2017)118 [arXiv:1611.04650 [hep-th]].

- [5] A. Larzul, A. M. Sengupta, A. Georges and M. Schirò, “Fast Scrambling at the Boundary,” [arXiv:2407.13617 [cond-mat.str-el]].
- [6] Y. Hatsugai, and M. Kohmoto, “Exactly Solvable Model of Correlated Lattice Electrons in Any Dimensions,” J. Phys. Soc. Jpn. **61**, 2056-2069 (1992) doi:10.1143/JPSJ.61.2056
- [7] D. Manning-Coe and B. Bradlyn, “Ground state stability, symmetry, and degeneracy in Mott insulators with long-range interactions,” Phys. Rev. B **108**, no.16, 165136 (2023) doi:10.1103/PhysRevB.108.165136 [arXiv:2306.00221 [cond-mat.str-el]].
- [8] M. V. Berry, “Semi-Classical Mechanics in Phase Space: A Study of Wigner’s Function,” Phil. Trans. Roy. Soc. Lond. A **287**, 237-271 (1977) doi:10.1098/rsta.1977.0145
- [9] F. J. Dyson, “Statistical theory of the energy levels of complex systems. I,” J. Math. Phys. **3**, 140-156 (1962) doi:10.1063/1.1703773
- [10] A. M. García-García, B. Loureiro, A. Romero-Bermúdez and M. Tezuka, “Chaotic-Integrable Transition in the Sachdev-Ye-Kitaev Model,” Phys. Rev. Lett. **120**, no.24, 241603 (2018) doi:10.1103/PhysRevLett.120.241603 [arXiv:1707.02197 [hep-th]].
- [11] M. V. Berry, “Regular and irregular semiclassical wavefunctions,” J. Phys. A **10**, no.12, 2083 (1977) doi:10.1088/0305-4470/10/12/016
- [12] S. Muller, S. Heusler, P. Braun, F. Haake and A. Altland, “Semiclassical foundation of universality in quantum chaos,” Phys. Rev. Lett. **93**, 014103 (2004) doi:10.1103/PhysRevLett.93.014103 [arXiv:nlin/0401021 [nlin.CD]].

- [13] O. Bohigas, M. J. Giannoni and C. Schmit, “Characterization of chaotic quantum spectra and universality of level fluctuation laws,” *Phys. Rev. Lett.* **52**, 1-4 (1984) doi:10.1103/PhysRevLett.52.1
- [14] Y. Y. Atas, E. Bogomolny, O. Giraud and G. Roux, “Distribution of the Ratio of Consecutive Level Spacings in Random Matrix Ensembles,” *Phys. Rev. Lett.* **110**, no.8, 084101 (2013) doi:10.1103/PhysRevLett.110.084101
- [15] W. Kirkby, D. H. J. O’Dell and J. Mumford, “False signals of chaos from quantum probes,” doi:10.1103/PhysRevA.104.043308 [arXiv:2108.09391 [quant-ph]].
- [16] E. Brézin and S. Hikami, “Spectral form factor in a random matrix theory,” *Phys. Rev. E* **55**, no.4, 4067 (1997) doi:10.1103/PhysRevE.55.4067
- [17] E. Dyer and G. Gur-Ari, “2D CFT Partition Functions at Late Times,” *JHEP* **08**, 075 (2017) doi:10.1007/JHEP08(2017)075 [arXiv:1611.04592 [hep-th]].
- [18] K. Okuyama, “Spectral form factor and semi-circle law in the time direction,” *JHEP* **02**, 161 (2019) doi:10.1007/JHEP02(2019)161 [arXiv:1811.09988 [hep-th]].
- [19] P. H. C. Lau, C. T. Ma, J. Murugan and M. Tezuka, “Randomness and Chaos in Qubit Models,” *Phys. Lett. B* **795**, 230-235 (2019) doi:10.1016/j.physletb.2019.05.052 [arXiv:1812.04770 [hep-th]].
- [20] P. H. C. Lau, C. T. Ma, J. Murugan and M. Tezuka, “Correlated disorder in the SYK₂ model,” *J. Phys. A* **54**, no.9, 095401 (2021) doi:10.1088/1751-8121/abde77 [arXiv:2003.05401 [hep-th]].
- [21] T. Xu, T. Scaffidi and X. Cao, “Does scrambling equal chaos?,” *Phys. Rev. Lett.* **124**, no.14, 140602 (2020) doi:10.1103/PhysRevLett.124.140602 [arXiv:1912.11063 [cond-mat.stat-mech]].
- [22] J. Maldacena, S. H. Shenker and D. Stanford, “A bound on chaos,” *JHEP* **08**, 106 (2016) doi:10.1007/JHEP08(2016)106 [arXiv:1503.01409 [hep-th]].

- [23] S. Ozaki and H. Katsura, “Disorder-free Sachdev-Ye-Kitaev models: Integrability and a precursor of chaos,” [arXiv:2402.13154 [cond-mat.str-el]].
- [24] D. A. Trunin, “Refined quantum Lyapunov exponents from replica out-of-time-order correlators,” *Phys. Rev. D* **108**, no.10, 105023 (2023) doi:10.1103/PhysRevD.108.105023 [arXiv:2308.02392 [hep-th]].
- [25] D. Marković and M. Čubrović, “Detecting few-body quantum chaos: out-of-time ordered correlators at saturation,” *JHEP* **05**, 023 (2022) doi:10.1007/JHEP05(2022)023 [arXiv:2202.09443 [hep-th]].